

Multi-scale modeling of diffusion-controlled reactions in polymers: Renormalisation of reactivity parameters

Ralf Everaers and Angelo Rosa

Citation: *J. Chem. Phys.* **136**, 014902 (2012); doi: 10.1063/1.3673444

View online: <http://dx.doi.org/10.1063/1.3673444>

View Table of Contents: <http://jcp.aip.org/resource/1/JCPSA6/v136/i1>

Published by the [American Institute of Physics](#).

Related Articles

Stochastic simulation of chemically reacting systems using multi-core processors

J. Chem. Phys. **136**, 014101 (2012)

Theoretical study of the aqueous solvation of HgCl₂: Monte Carlo simulations using second-order Moller-Plesset-derived flexible polarizable interaction potentials

J. Chem. Phys. **136**, 014502 (2012)

Exact on-lattice stochastic reaction-diffusion simulations using partial-propensity methods

J. Chem. Phys. **135**, 244103 (2011)

An ab initio quasi-diabatic potential energy matrix for OH(2) + H₂

J. Chem. Phys. **135**, 234307 (2011)

Modelling charge transfer reactions with the frozen density embedding formalism

J. Chem. Phys. **135**, 234103 (2011)

Additional information on *J. Chem. Phys.*

Journal Homepage: <http://jcp.aip.org/>

Journal Information: http://jcp.aip.org/about/about_the_journal

Top downloads: http://jcp.aip.org/features/most_downloaded

Information for Authors: <http://jcp.aip.org/authors>

ADVERTISEMENT

AIPAdvances

Submit Now

Explore AIP's new
open-access journal

- Article-level metrics now available
- Join the conversation! Rate & comment on articles

Multi-scale modeling of diffusion-controlled reactions in polymers: Renormalisation of reactivity parameters

Ralf Everaers^{1,a)} and Angelo Rosa^{2,b)}

¹Laboratoire de Physique and Centre “Blaise Pascal,” Ecole Normale Supérieure de Lyon, Centre National de la Recherche Scientifique UMR 5672, Université de Lyon, 46 Allée d’Italie, 69634 Lyon Cedex 07, France

²Sissa (Scuola Internazionale Superiore di Studi Avanzati) and Italian Institute of Technology (Sissa unit), Via Bonomea 265, 34136 Trieste, Italy

(Received 7 August 2011; accepted 6 December 2011; published online 4 January 2012)

The quantitative description of polymeric systems requires hierarchical modeling schemes, which bridge the gap between the atomic scale, relevant to chemical or biomolecular reactions, and the macromolecular scale, where the longest relaxation modes occur. Here, we use the formalism for diffusion-controlled reactions in polymers developed by Wilemski, Fixman, and Doi to discuss the renormalisation of the reactivity parameters in polymer models with varying spatial resolution. In particular, we show that the adjustments are independent of chain length. As a consequence, it is possible to match reactions times between descriptions with different resolution for relatively short reference chains and to use the coarse-grained model to make quantitative predictions for longer chains. We illustrate our results by a detailed discussion of the classical problem of chain cyclization in the Rouse model, which offers the simplest example of a multi-scale descriptions, if we consider differently discretized Rouse models for the same physical system. Moreover, we are able to explore different combinations of compact and non-compact diffusion in the local and large-scale dynamics by varying the embedding dimension. © 2012 American Institute of Physics. [doi:10.1063/1.3673444]

I. INTRODUCTION

The dynamics of intra- and inter-macromolecular chemical reactions is a classical problem of polymer physics, which stimulated intense theoretical,^{1–17} computational,^{18–20} and experimental (DNA looping,^{21,22} protein,^{23–30} and RNA folding^{31,32}) work over the last 40 years. Theoretical work typically concentrates on exploring the reaction dynamics of model polymers. There are now increasing efforts to systematically develop hierarchies of coarse-grain models describing the structure and dynamics of a polymeric system on different time and length scales.^{33–43} In the present paper, we discuss the renormalisation of reactivity parameters required to obtain consistent results from models with different spatial resolution.

For intra- or inter-molecular reactions to occur, the reactive sites have to come into close spatial contact. Depending on the efficiency of the chemical reaction, two qualitatively different regimes exist. If the reaction is inefficient, the reactive sites have to approach each other very often before a reaction occurs. The rate, τ_{rc}^{-1} , of reaction-controlled or reaction-limited processes is therefore independent of the chain dynamics and given by the product of two factors: (i) the static probability, p_c , that the chain folds into a conformation, where the reactive sites approach within a microscopic contact distance, r_c , and (ii) the rate $\lambda(r_c)$ with which reactive sites confined to the contact volume undergo the chemical reaction in question. In the opposite limit of diffusion-controlled reactions, two chain ends interact each time they come closer than

r_c . In this limit, the reaction time is given by the mean first-contact time, τ_{dc} , of the reactive sites and is hence a function of the chain dynamics. In the present paper, we are interested in what can be learned about τ_{dc} from coarse-grain polymer models.

The character of diffusion-controlled processes sensitively depends on the embedding spatial dimension, d , and, as a measure of the chain dynamics, on the exponent, z , describing the mean square variations in the distance $\vec{r}(t)$ between the reactive sites, $\langle(\vec{r}(t) - \vec{r}(0))^2\rangle \sim t^z$. In the following, we denote by $\tau_{\min} \sim r_c^{2/z}$ the time it takes to diffuse a distance of the order of the reaction distance, r_c . Similarly, the maximal relaxation time is given by the time $\tau_{\max} \sim R^{2/z}$ required to diffuse across the total accessible volume, R^d . For non-compact diffusion⁷ with $dz > 2$ the regions $\sim T^{dz/2}$ explored by \vec{r} during two subsequent time intervals of length T do not overlap. As a consequence, the diffusive process has to visit on average $1/p_c \sim (R/r_c)^d$ cells of the size of the contact volume before it will by chance enter the reaction volume itself. The required time scales such as $\tau_{dc} \sim \tau_{\min} p_c^{-1} = \tau_{\max} p_c^{2/(dz)-1} \gg \tau_{\max}$. For compact diffusion⁷ with $dz < 2$ spatial volumes visited during subsequent time intervals are densely overlapping and a trajectory passes arbitrarily close to any point within the explored range $T^{dz/2}$. “Targets” in finite systems are thus found independently of their size in a time corresponding to the overall relaxation time of the system, $\tau_{dc} = \tau_{\max}$. The transition from compact to non-compact regime defines the “critical” dimension, $d_c = 2/z$.

These general considerations are best illustrated by the example of simple diffusion, $\langle(\vec{r}(t) - \vec{r}(0))^2\rangle \sim Dt$, in a finite volume R^d . In this case, $z = 1$ and $d_c = 2$: diffusion is compact for $d < 2$ and non-compact for $d > 2$, with

^{a)}Electronic mail: ralf.everaers@ens-lyon.fr.

^{b)}Electronic mail: anrosa76@gmail.com.

$\tau_{dc} = \tau_{max} \approx R^2/D$ independent of r_c for $d = 1$, and $\tau_{dc} \approx R/r_c \tau_{max} = R^3/Dr_c$ for $d = 3$ in agreement with the classical result by Smoluchowski.⁴⁴

Depending on solvent quality, concentration and the degree of screening of hydrodynamic interactions, macromolecular systems exhibit a rich variety of non-trivial exponents giving rise to both, compact, and non-compact diffusion. Let us consider two monomers located at contour length positions i and j from one chosen end of the fiber. For flexible chains with a conformational statistics described by the average square spatial distance $\langle r^2(|i - j|) \rangle \sim |i - j|^{2\nu}$, and neglecting hydrodynamics interactions, the internal dynamics is described by the Rouse model,^{45,46} where $z = 2\nu/(2\nu + 1)$. For ideal chains $\nu = 1/2$, while for self-avoiding polymers $\nu = 3/(d + 2)$ is the Flory exponent.⁴⁷ Thus, both models exhibit the transition from compact to non-compact dynamics at the “critical” dimension $d = d_c = 4$. Inclusion of hydrodynamic interactions in the Zimm model⁴⁸ yields $z = 2/3$ and $d_c = 3$, while for stiff chains, $z = 3/4$ and $d_c = 8/3 < 3$. Beyond the maximal relaxation of the chains, motion is also characterized by the non-compact (in $d > 2$) center-of-mass diffusion.⁷

A given system may exhibit different dynamic regimes on different time and length scales.^{49–52} While complex, most of these properties can be reproduced by a hierarchy of models hiding molecular specificity in a small number of parameters accounting for the chain topology, conformational statistics, or the effective interactions. Since the calculation of diffusion-controlled reactivity potentially involves all length and time scales, it presents a considerable challenge to this paradigm, even if the dynamics is apparently dominated by a single scaling regime.

Naively, one would expect coarse-graining to be uncritical in cases where both the true system (or a suitable microscopic model) and the coarse grain model exhibit compact diffusion at *all* times. In contrast, omitting a non-compact regime of the microscopic dynamics or (involuntarily) introducing such a regime in the coarse-grain dynamics is bound to lead to seriously flawed results, even if the long-time dynamics is explored correctly. As we will show later, the arising difficulties can be readily illustrated using the standard example of ring-closure for flexible chains undergoing Rouse motion, which has been a recurrent subject in the literature since the earliest publications in the field.^{2,3,6} The existence of different scaling regimes with $\tau_{dc} \sim N^{3/2}$ and $\tau_{dc} \sim N^2$ for this standard model of polymer dynamics is by now well established.^{11,13,53} As their relative importance (and the characteristic chain length where the crossover between them occurs) turn out to depend on the reaction radius and the microscopic discretization used for the polymer model, this raises the problem of how to map the results to real systems and how to represent real systems by polymer models.

In the present paper, we explore the use and the limitations of coarse-grain models for estimating diffusion limited reactivities in polymeric systems.

In Sec. II, we review the classical theory of Wilemski and Fixman¹ in a simplified form suggested by Doi⁵ from this particular angle.

In Sec. III, we present a detailed analysis of numerical results for the Rouse model as a function of chain length, spatial resolution of the model, and embedding dimension. Our main interest is in describing a simple regularization procedure allowing the separation of local and polymer contributions to the reaction time, which provides a transparent physical interpretation for the scaling regimes mentioned above.

Based on these results, the discussion in Sec. IV focuses on the standard questions of polymer physics:^{46,47,54–56}

1. For everything else left unchanged, how does the reaction time, τ_r vary with the total chain length, L , or the contact distance between the reactive sites? By L , we refer to a measure of the size of the real polymer, which we are trying to model. Examples would be the contour length, the molecular weight, or the index of polymerization.
2. What is the predictive power of polymer models and how should we analyze their behavior to obtain robust results? While we use the Rouse model throughout the paper to illustrate our results, we are neither trying to solve it with higher precision^{15,16} than the classical authors^{1,5} nor are we suggesting that all polymers are suitably described by a simple Langevin dynamics of Gaussian chain. Instead, we use the Wilemski, Fixman, and Doi theory for the Rouse model to *illustrate* the consequences of investigating the reaction dynamics of a particular polymer *using models with different spatial resolution*. In our notation, the number of beads, N , of a Rouse chain is, therefore, not simply synonymous to the length, L , of the molecule under investigation. Instead, $N = N_0(L/L_0)$, where L_0 is a reference chain length and where N_0 is a measure of the chosen spatial discretization. Different models differ only in their behavior on the smallest resolved length and time scales and make nearly indistinguishable predictions for quantities such as the solution viscosity (Fig. 5). However, there are significant effects on the first-contact time (Fig. 4). This observation is equally relevant to analytical and numerical attempts to predict reaction times.
3. How can we integrate independent information about *microscopic* behavior into (the parameters of) a coarse-grain model to generate the correct behavior? We discuss strategies for compensating the consequences of a modified short-time dynamics in a model by adjusting the employed reactivity parameters. In particular, we show that changes of resolution can be performed without loss of predictive power, since the new values for the contact distance, r_c , and the conversion rate at contact, λ , are independent of chain length.

Finally, it is probably worthwhile to comment on our use of the term “quantitative” in this paper. We are interested in predicting the chain length dependence of reaction rates, $\tau_r(L)$, for polymers of given chemical composition under given environmental conditions. These reaction rates vary over many orders of magnitude and often exhibit power law behavior. By “quantitative,” we mean the determination of prefactors and crossovers within $\sim 15\%$ (see Fig. 1 in supplementary material), i.e., better than scaling, but not exact.

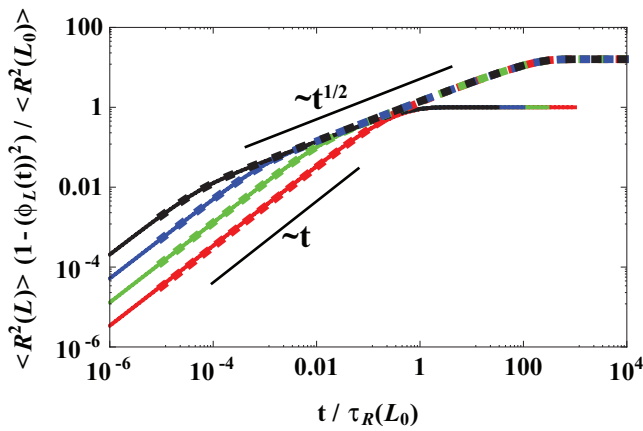


FIG. 1. Time-dependence of the variance $1 - \phi^2(t)$ of the Green function for the end-to-end vector in the Rouse model. Solid lines show results for a reference chain with longest relaxation (Rouse) time $\tau_R(L_0)$ and size $R^2(L_0)$ for $N = 4$ (red), $N = 16$ (green), $N = 64$ (blue), and $N = 256$ (black). Thick dashed lines show results for a correspondingly discretized, longer chain with $L/L_0 = 16$.

II. THEORY

A. Mean first-contact times and contact correlation functions

Consider a polymer of contour length L with reactive sites located at chain ends. Neglecting orientational effects, the contact, or looping probability is given by

$$p_c(L, r_c) = \int_{\vec{r} \in \mathcal{S}(r_c)} p_L(\vec{r}) d\vec{r}, \quad (1)$$

where $p_L(\vec{r})$ is the probability density for the spatial vector between the reactive sites being \vec{r} , and the integral is calculated over the “reaction region” \mathcal{S} of linear size the “contact distance” r_c .

Calculating the average reaction time between two sites on a polymer undergoing Brownian motion is a non-trivial statistical mechanical problem. In their seminal paper,¹ Wilemski and Fixman (WF) laid out the mathematical framework for the solution of the first-contact problem for two diffusing reactive sites on a polymer. Their approach is based on a “Markovian” approximation of the exact solution^{15,16} to the cyclization problem of a polymer chain, and predicts mean-first contact times fairly close to the exact result (see Ref. 15 and Fig. 1 in supplemental material⁵⁷). The full WF solution for arbitrary conversion rates λ for reactive sites in contact relies on Laplace transformations. Here, we will use an approximation proposed by Doi,⁵ which we find particularly transparent as to the underlying physics.

Doi⁵ showed that a lower bound on the average reaction time τ_r is given by the sum

$$\tau_r \geq \tau_{rc} + \tau_{dc} \quad (2)$$

of two reaction times describing the limits of reaction- and a diffusion-controlled processes, respectively. The first term

$$\tau_{rc} = \frac{\lambda^{-1}}{p_c} \quad (3)$$

is calculated in the limit $\lambda \rightarrow 0$, where the concentration of unreacted chains with reactive sites in contact is indeed given by the *equilibrium* contact probability, Eq. (1). Chemical reactions deplete the concentration of these conformations so that τ_{rc} underestimates τ_r for finite conversion rates. The extreme case is given by the limit $\lambda \rightarrow \infty$, where Eq. (2) becomes again exact. In particular, Doi proposed to calculate τ_{dc} from the more easily accessible average contact time, τ_S ,

$$\tau_{dc} = \frac{\tau_S}{p_c}, \quad (4)$$

where

$$\tau_S = \left\langle \int_0^\infty [S(r(t)) - p_c] dt \right\rangle_c \quad (5)$$

$$\equiv \int_0^\infty [\Sigma(t) - p_c] dt. \quad (6)$$

The *sink* function S introduced above is the characteristic function of the reaction region \mathcal{S} :⁵⁸ it takes the value one each time the two interacting monomers are closer than r_c and 0 otherwise. The brackets $\langle \dots \rangle_c$ denote the average over the ensemble of trajectories for which $r(t) < r_c$ at $t = 0$.

To better understand the meaning of the function $\Sigma(t) \equiv \langle S(r(t)) \rangle_c$, we note that the contact probability is given by the ensemble average of the characteristic function, $p_c \equiv \langle S \rangle \equiv \langle S^2 \rangle$. Therefore, the average over the ensemble of trajectories passing through the contact region at $t = 0$ can also be written as $\langle \dots \rangle_c \equiv \langle \dots S(r(t=0)) \rangle / p_c$ so that, by adopting the concise notation $S(t) \equiv S(r(t))$,

$$\Sigma(t) = \frac{\langle S(t)S(0) \rangle}{p_c} \quad (7)$$

turns out to be the contact correlation function. By construction, $\langle S^2(0) \rangle = p_c$ and $\Sigma(0) = 1$. Furthermore, $\lim_{t \rightarrow \infty} \langle S(t)S(0) \rangle = \langle S(t) \rangle \langle S(0) \rangle = p_c^2$ and $\lim_{t \rightarrow \infty} \Sigma(t) = p_c$, so that the integral, Eq. (6) converges.

It is instructive, to consider the integration of $\Sigma(t)$ (Eq. (6)), in the context of our discussion of compact and non-compact diffusion in the Introduction, Sec. I. The decay of $\Sigma(t)$ remains suspended during an initial time interval, $0 < t < \tau_{\min} = (r_c/R)^{2/z} \tau_{\max}$ required to diffuse out of the contact volume: $\int_0^{\tau_{\min}} \Sigma(t) dt = \tau_{\min}$ may be neglected. Since $\Sigma(t)$ is also a measure of the “probability” for the interacting particles to return inside the contact region and $\langle (\vec{r}(t) - \vec{r}(0))^2 \rangle \sim t^z$ for $\tau_{\min} < t < \tau_{\max}$, $\Sigma(t)$ is expected to decay as a power-law: $\Sigma(t) \sim (t/\tau_{\min})^{-dz/2}$. Hence,

$$\tau_S \approx \int_{\tau_{\min}}^{\tau_{\max}} \frac{1}{(t/\tau_{\min})^{dz/2}} dt \approx \begin{cases} p_c \tau_{\max}, & \frac{dz}{2} < 1 \\ \tau_{\min} \log\left(\frac{1}{p_c}\right), & \frac{dz}{2} = 1 \\ \tau_{\min}, & \frac{dz}{2} > 1 \end{cases} \quad (8)$$

which, when combined with Eq. (4), leads back to results for τ_{dc} discussed in the Introduction.

More formally, because the sink function $S(\vec{r})$ depends only on the distance between the reactive sites, $\Sigma(t)$ is related to the Green function $G(\vec{r}, t|\vec{r}_0, 0)$ for that distance^{1,2}

$$\Sigma(t) = p_c^{-1} \int d\vec{r} \int d\vec{r}_0 S(\vec{r}) G(\vec{r}, t|\vec{r}_0, 0) S(\vec{r}_0) p_L(\vec{r}_0). \quad (9)$$

The Green function gives the conditional probability density that, for a reciprocal spatial position \vec{r}_0 at time $t = 0$ the vector between the two reactive sites at time t is \vec{r} .

B. Rouse model

The different ideas raised in Sec. II A can be readily illustrated using the classical example of intrachain reactions in flexible polymers^{2,3,9} in d dimensions. The Rouse model^{45,46} is the standard theoretical framework for flexible polymer dynamics: the chain is described as a linearly connected array of $N + 1$ beads linked by Gaussian springs. The model does not take into account hydrodynamic interactions, and because of its simplicity it is exactly solvable.^{45,46} Here, we consider a slightly modified model, where the friction coefficient of the first and the last bead of the chain is only half as large as for the inner beads. This choice is motivated by the construction of longer chains via the polymerization of Rouse dimers or dumbbells. As a consequence, the total friction scales as the number of *bonds*, N , and the dispersion relation for the discrete model equals the well-known results in the continuum limit and avoids various “ $1/N$ ” corrections of the standard Rouse model (Appendix A). By assuming a simple, analytical expression for the sink function in Eq. (9), the contact correlation function $\Sigma(t)$ is given by the *exact* expression (Appendix B),

$$\Sigma(t) = \frac{p_c}{[(1 - p_c^{2/d})(1 - \phi^2(t)) + p_c^{2/d}]^{d/2}}, \quad (10)$$

where

$$\phi(t) = \frac{4}{N^2} \sum_{p=1, \text{ odd}}^{N-1} \frac{\exp\left(-\frac{t}{\tau_p}\right)}{1 - \cos\left(\frac{p\pi}{N}\right)}, \quad (11)$$

with $\tau_p = \tau_R(1 - \cos(\frac{p\pi}{N})) / (1 - \cos(p\pi/N))$ and τ_R is the so-called Rouse time of the chain. For $t < \tau_{N-1}$, it is easy to show that

$$\phi(t) \approx 1 - \frac{2}{N \left[1 - \cos\left(\frac{\pi}{N}\right)\right]} \frac{t}{\tau_R}. \quad (12)$$

Hence, at short enough times, monomer motion is always diffusive. We will show in Sec. III, that this has important effects reverberating on contact times.

III. RESULTS

A. The origin of the different scaling regimes in the Rouse model

It is a simple numerical exercise to evaluate Eq. (4) with Eqs. (6), (10), and (11), for the Rouse model for given values of contact radius, r_c , Rouse time, τ_R , and root-mean square chain extension, R . In the following, we vary chain length,

L , and the number of beads, N , used to represent the chain, in an attempt to trace their influence on the final result. We use the shortest chains studied as a reference and the corresponding values of τ_R^0 , R_0 , and L_0 as our units of time, length, and chain length. In the figures, different colors denote results obtained for different spatial discretizations with $N_0 = 4, 16, 64, 256$ beads for the reference chain and with $N = N_0(L/L_0)$ beads for longer chains. For Rouse chains: $R = R_0(L/L_0)^{1/2}$, $\tau_R = \tau_R^0(L/L_0)^2$, and contact probabilities are given (for $r_c \ll R_0$) by $p_c(L_0) = (d/2)^{d/2} / \Gamma(d/2 + 1) (r_c/R_0)^d$ (Appendix B) and $p_c(L) = p_c(L_0)(L_0/L)^{d/2}$.

Because of the evident importance of this specific case, we trace the physical origin of the two regimes observed in $d = 3$ (Refs. 11, 13, and 53) by going step-by-step through the Doi formalism.

As we have seen in Sec. II B, the information about the chain dynamics enters into the formalism via the time-dependent variance, $1 - \phi^2(t)$, of the Green function for the end-to-end vector (Appendix B). In Fig. 1, we show this quantity for a reference chain of length L_0 and a longer chain of length $L = 16L_0$. Around the terminal relaxation time, $\tau_R(L) \sim L^2$, the variance $1 - \phi^2(t)$ is independent of the discretization of the model. In contrast, the characteristic crossover from free diffusion, $1 - \phi^2(t) \sim t$, to Rouse dynamics, $1 - \phi^2(t) \sim t^{1/2}$, occurs independently of chain length on time scales corresponding to the relaxation time, τ_{N-1} , of the highest mode represented in the polymer model. Note that while $t^{1/2}$ grows more slowly in time than t , the absolute magnitude of motion is *increased* by the introduction of thermally fluctuating microscopic degrees of freedom. Being thus more efficient in the exploration of space, Rouse dynamics is *compact* in $d = 3$ dimensions. Nevertheless, a Rouse chain with finite discretization exhibits *non-compact* diffusion for $t < \tau_{N-1}$ (Eq. (12)). In our figures, τ_{N-1} is identical for chains of different lengths shown in the same color.

Figure 2 shows the contact correlation function, $\Sigma(t) - p_c$, calculated from Eq. (10) for the same chains of length L_0 and $16L_0$ for three different values of $r_c/R(L_0)$. $\Sigma(t) \approx 1$ as long as $\sqrt{1 - \phi^2(t)} < r_c/R(L_0)$. Obviously, the larger r_c , the longer this regime becomes. Comparing results for

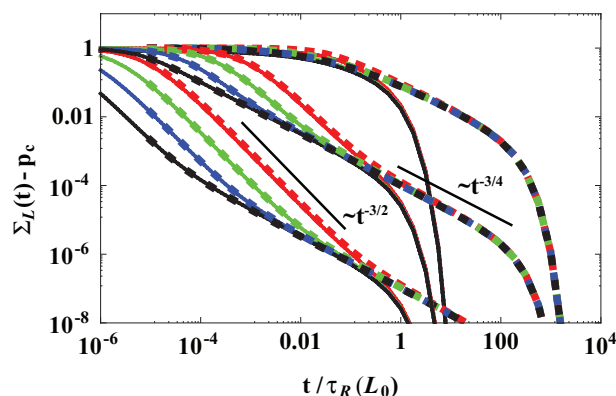


FIG. 2. Correlation function for contacts between the end beads in the Rouse model for $r_c/\sqrt{R^2(L_0)} = 0.5, 0.05, 0.005$ (from top to bottom) for the differently discretized chains from Fig. 1, for chain length L_0 (thin, solid lines) and $16L_0$ (thick, dashed lines) and $d = 3$.

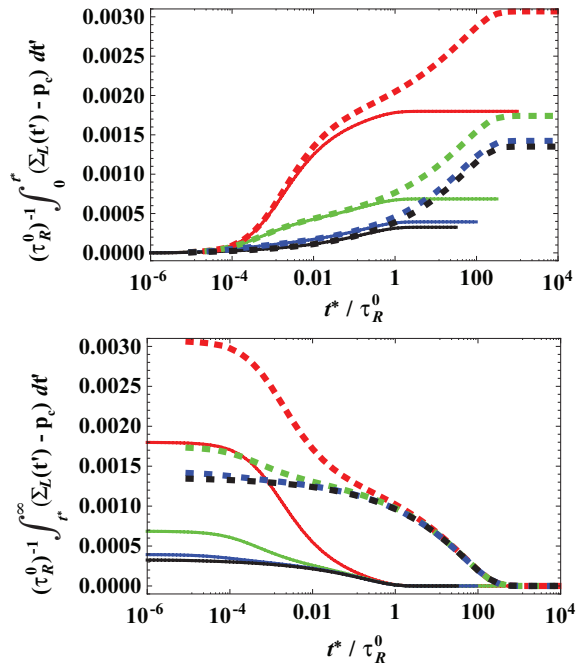


FIG. 3. Partial integrals over the contact correlation functions from Fig. 2 for $r_c/\sqrt{R^2(L_0)} = 0.05$. Results are shown for chains of length L_0 (thin, solid lines) and $16L_0$ (thick, dashed lines) and $d = 3$. Different colors denote different discretization (see Fig. 1).

different discretization, we see that the decay of $\Sigma(t)$ sets in much earlier in faster moving systems with many microscopic degrees of freedom. In the intermediate regime before the terminal decay at the Rouse time, $\tau_R(L)$, we clearly discern two different power laws, $\Sigma(t) \sim t^{-3/2}$ and $\Sigma(t) \sim t^{-3/4}$, corresponding to non-compact and compact diffusion below and above the relaxation time, τ_{N-1} , of the highest mode represented in the polymer model. For times $t < \tau_R^0$, longer chains perfectly reproduce the behavior of corresponding reference chains. In the opposite limit, $\tau_R^0 < t$, the behavior of long chains is independent of discretization.

The contact time, τ_S , is calculated by integrating $\Sigma(t) - p_c$ over time, Eq. (6). In Fig. 3, we show partial integrals to illustrate how different time intervals and regimes contribute to τ_S . The figure suggests to write τ_S as a sum of two qualitatively different contributions:

$$\tau_S(L) = \tau_S^{\text{micro}} + \tau_S^{\text{pol}}(L) \quad (13)$$

with $\tau_S^{\text{micro}}(L, t^*) = \int_0^{t^*} [\Sigma_L(t) - p_c] dt$ and $\tau_S^{\text{pol}}(L, t^*) = \int_{t^*}^{\infty} [\Sigma_L(t) - p_c] dt$ for some appropriate cut-off time, which we choose in the following as $t^* = 0.01\tau_R^0$.

The asymptotically dominant long-time contribution, $\tau_S^{\text{pol}}(L)$, is independent of discretization and a manifestation of the universal, large-scale polymer *dynamics*. The chain length dependence of $\tau_S^{\text{pol}}(L)$ is indicated by the superimposed dashed lines in Fig. 3 (bottom). With Rouse motion being *compact* in three dimensions, $\tau_S^{\text{pol}}(L)$ is essentially given by $p_c \tau_R(L)$. As a consequence, $\tau_{\text{dc}}^{\text{pol}}(L) \sim \tau_R(L) \sim L^2$. In fact, by careful numerical evaluation we find that $\tau_{\text{dc}}^{\text{pol}}(L)/\tau_R(L)$ is ≈ 2 , in agreement with previous findings.^{2,9,10}

In contrast, the short-time contribution, τ_S^{micro} , is a function of discretization and *independent* of chain length (compare dashed and solid lines, Fig. 3 (top)). Large contributions from the short-time regime are a consequence of local *non-compact* diffusion in systems with finite discretization. Around the time of the crossover, τ_{N-1} , of the “monomer” motion from simple diffusion to Rouse dynamics, their typical mean-square displacement is of the order of $R^2(L)/N$. For $r_c^2 > R^2(L)/N$ the finite discretization is of no consequence and, the relevant short-time dynamics is compact: hence, analogously to the derivation of Eq. (8), and with $\tau_{\text{max}} = \tau_R(L)$, $z = 1/2$, and $d = 3$ it is easy to show that $\tau_S^{\text{micro}} \approx p_c \tau_R(t^*/\tau_R)^{1/4} \approx \tau_{\text{min}}^{3/4} t^{*1/4}$. In the opposite case, τ_S^{micro} is dominated by the time required to escape from the contact volume via simple, *non-compact* diffusion, $\tau_S^{\text{micro}} = (r_c^2/R^2)\tau_R(L)/N \approx (r_c^2/D)L^0$, where D is the monomer diffusion coefficient. Then, the corresponding contribution to τ_{dc} scales like $\tau_{\text{dc}} \approx \tau_S^{\text{micro}}/p_c \approx R^3/r_c D \sim L^{3/2}$ as a consequence of the decreasing *static* contact probability, $p_c(L, r_c)$ between the reactive sites.

B. Reaction times as a function of chain discretization and spatial dimension

We can now generalize these results to different dimensions. Figure 4 shows the behavior of $\tau_S(L)$ and $\tau_{\text{dc}}(L)$ as a function of chain length, for $d = 1, 3, 4, 5$. The symbols show numerical results obtained for $r_c = 0.01R_0$. Dotted and dashed lines denote specific contributions from the model (discretization dependent) short-time behavior and the universal (polymer) behavior, respectively. For $d = 1$, both diffusion and Rouse behavior are compact. Consequently, model coarsening has little effect and the polymer (universal) contribution dominates. For $d = 3$, we come back to the case discussed in Sec. III A: diffusion is non-compact, while Rouse motion is still compact. Accordingly, the data reproduce the well-known crossover^{11,13,53} from a scaling regime with $\tau_{\text{dc}}(L) \sim L^{3/2}$ to an asymptotic regime $\tau_{\text{dc}}(L) \sim \tau_R(L) \sim L^2$.^{3,9,10} As discussed above, while the former strongly depends on the chosen discretization of the model, the latter is universal. For $d = 4$ (i.e., the *marginal* case of the Rouse model), we observe the predicted (slow) logarithmic behavior of $\tau_S^{\text{pol}}(L)$ at large L (see Eq. (8)). It is noticed that the dominant numerical contribution to $\tau_S(L)$ comes from τ_S^{micro} . Finally, for $d = 5$ both diffusion and Rouse motion are non-compact. Accordingly, we report no crossover: only the $\sim L^{5/2}$ regime is observed, with the dominant contribution coming from τ_S^{micro} .

Within the Rouse model, it depends on chain length, L , the discretization, N , the contact radius, r_c , and the spatial dimension, d , whether the contact correlation time τ_S is dominated by the universal contribution, τ_S^{pol} , or the non-universal contribution, τ_S^{micro} . This raises the question, if we are dealing with a real physical effect or with an artifact. It is tempting to dismiss the asymptotically sub-dominant contribution on the grounds that the universal behavior is typically all that matters in polymer physics. This point of view most certainly simplifies calculations. Adopting it in numerical work, the sub-dominant contribution would appear as a nuisance imposed by the need to employ finite contact radii and polymer

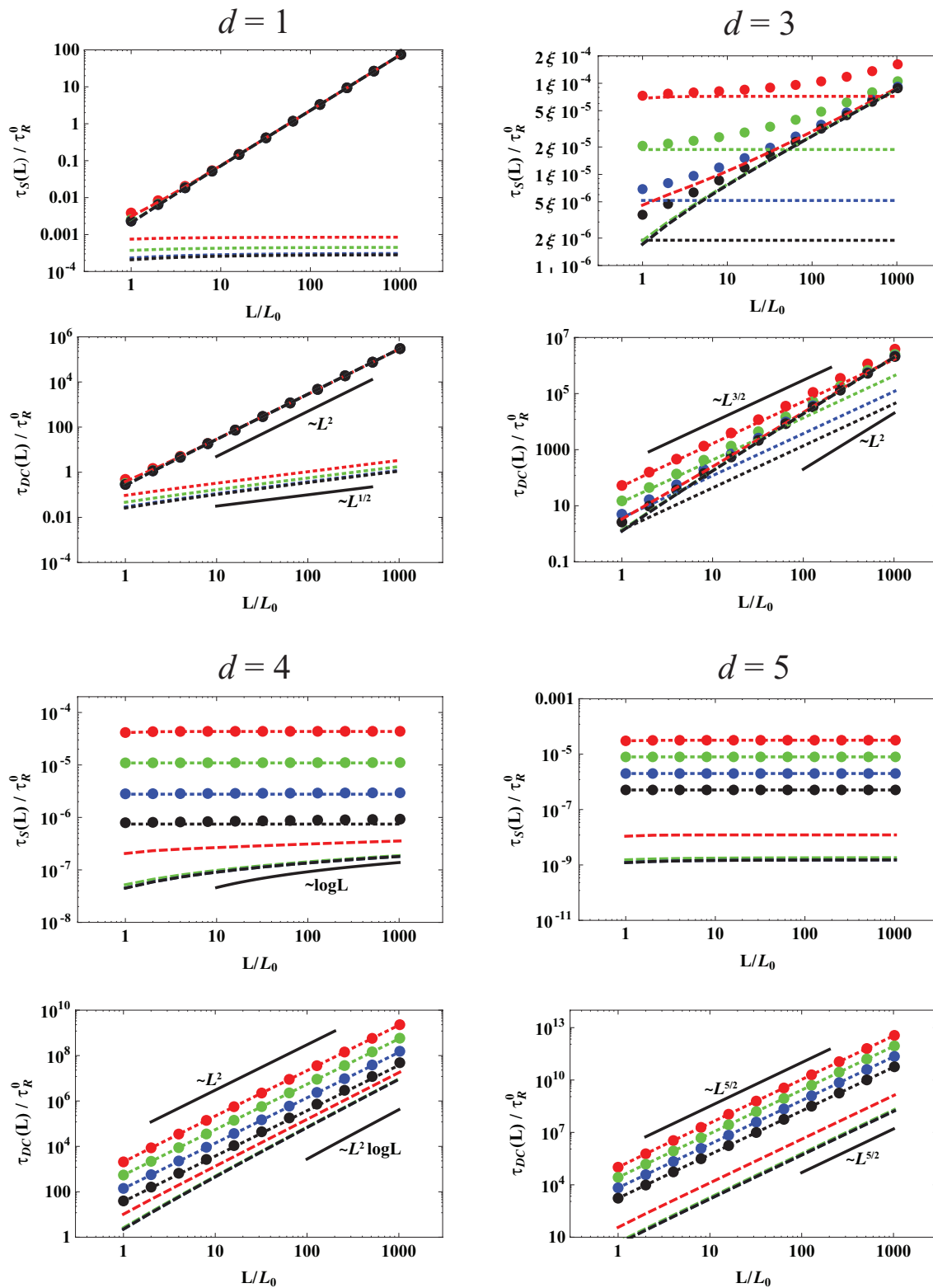


FIG. 4. Contact correlation time, $\tau_S(L)$, and mean first contact times $\tau_{dc}(L) = \tau_S(L)/p_c(L, r_c)$, for Rouse chains as a function of chain length for contact radius, $r_c/R_0 = 0.01$, and for space dimension, $d = 1, 3, 4, 5$. The symbols indicate numerical results for $\tau_S(L) = \int_0^\infty [\Sigma(t) - p_c] dt$. Dotted lines show the model/discretization dependent short-time contribution, $\tau_S^{\text{micro}}(L) = \int_0^{0.01\tau_R^0} [\Sigma(t) - p_c] dt$, and dashed lines represent the universal contribution, $\tau_S^{\text{pol}}(L) = \int_{0.01\tau_R^0}^\infty [\Sigma(t) - p_c] dt$, from the long-time polymer dynamics (Eq. (13)). Different colors indicate different discretizations of the model with $N = N_0(L/L_0)$: $N_0 = 4$ (red), $N_0 = 16$ (green), $N_0 = 64$ (blue), $N_0 = 256$ (black). Notice, that results for $\tau_S^{\text{pol}}(L)$ generally superimpose for $N_0 \geq 16$. $d = 1$: Both diffusion and Rouse behavior are compact. Consequently, model coarsening has little effect and the polymer (universal) contribution dominates. $d = 3$: Diffusion is non-compact, while Rouse behavior is still compact. In this case, we reproduce the well-known crossover^{11,13,53} from a scaling regime with $\tau_{dc}(L) \sim L^{3/2}$ to an asymptotic regime $\tau_{dc}(L) \sim \tau_R(L) \sim L^{2,3,9,10}$. $d = 4$: In the Rouse marginal case, logarithmic corrections (Eq. (8)) are observable in the polymer contribution to $\tau_S(L)$. Dominant contributions come from the non-universal short-time behavior. $d = 5$: Both diffusion and Rouse behavior are non-compact, and only the short-time contribution matters.

models with a finite number of degrees of freedom. Fortunately, Fig. 3 would then suggest an efficient cure as the asymptotic behavior may be extracted from $\tau_S^{pol}(L)$ with minimal corrections to scaling. But is this attitude really justified, when it comes to modeling the behavior of real systems?

IV. MULTI-SCALE MODELING OF DIFFUSION LIMITED REACTIONS IN POLYMERS

A. Disregarding the model-dependent microscopic dynamics

In constructing a Rouse model of a specific flexible polymer, R^2 and τ_R are chosen to match the experimental mean-square end-to-end distance and longest relaxation time. The number of beads, N , is a free variable, which determines the chosen discretization. There are two natural choices: a discretization $N_K = L/l_K$ at the Kuhn scale, l_K , where rigid rod behavior crosses over to random walk behavior, and the continuum limit, $N \rightarrow \infty$, which is often convenient for analytical calculations, but which implies random walk behavior on all scales. Representations with $N < N_K$ beads are coarse-grained models. Apart from its simplicity, we have chosen the Rouse model as an example, because it allows for a convenient control of the renormalisation of the model parameters related to changes in spatial resolution.

Predictions for physical observables dominated by the large-scale (polymer) behavior are hardly affected by the choice of N . For comparison, it is useful to consider a concrete example: of the viscosity of polymer solutions. Quite analogous to Eqs. (6), (10), and (11), within the Rouse model⁴⁶ the viscosity is given by an integral over the shear relaxation modulus, $\eta = \int_0^\infty G(t) dt$, which in turn can be expressed as a sum over the correlation functions of the Rouse modes, $G(t) = \rho_{chain} k_B T \sum_{p=1}^N \exp(-t/\tau_p)$, where $\rho_{chain} = \rho_K(l_K/L) \sim L^{-1}$ for a given Kuhn segment density, ρ_K . The resulting prediction for the viscosity, $\eta(L) = \alpha(N) \rho_{chain}(L) k_B T \tau_R(L) \sim L^1$, depends on the discretization only through a numerical prefactor, $\alpha(N) = \sum_{p=1}^N \tau_p/\tau_1$, which rapidly converges with $\alpha(1) = 1$, $\alpha(4) \approx 1.61$, and $\alpha(\infty) = \pi^2/6 \approx 1.645$. In a log-log plot of viscosity versus chain length (Fig. 5), it is impossible to discern these small variations.

Coming back to the problem of diffusion-controlled reactions in polymeric systems, we see that the results presented in Sec. III B are somewhat alarming from a modeling perspective: With the exception of the 1d case (where both the local and global diffusions are compact), the resulting predictions for reaction times $\tau_{dc}(L)$ and $\tau_r(L, \lambda)$, shown in Figs. 4 and 6 respectively, strongly depend on the *ad hoc* choice of the discretization, N . To appreciate the magnitude of the problem, we invite the reader to gauge the spread in these predictions against the corresponding results for the viscosity shown in Fig. 5. Except in the asymptotic limit,⁹ the usual benign neglect of microscopic detail in polymer models fails: by themselves (i) the knowledge of the (chemical) conversion rate for reactive sites in contact and (ii) a reliable model of the large-scale structure and dynamics are insufficient to predict reaction rates in diffusion-controlled processes.

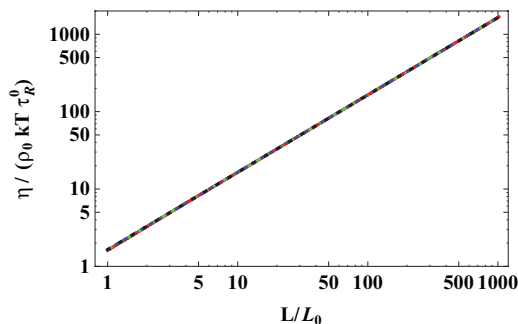


FIG. 5. Viscosity for Rouse chains as a function of chain length. The figure shows a superposition of four dashed lines representing results obtained for different discretizations of the model with $N = N_0(L/L_0)$: $N_0 = 4$ (red), $N_0 = 16$ (green), $N_0 = 64$ (blue), $N_0 = 256$ (black).

B. Universal and model-dependent contributions to τ_{dc}

The considerations in this paper build on the observation, that the short-time dynamics in polymers is independent of chain length. In particular, we propose to distinguish a *model-dependent, chain-length independent* short-time contribution, τ_S^{micro} , and a *universal, chain-length dependent* long-time contribution, $\tau_S^{pol}(L)$.

As a consequence, the integral Eq. (6) is amenable to a simple regularization procedure, where one calculates the change of the contact time for chains of length L relative to some appropriate reference chain length L_0 ,

$$\Delta\tau_S(L) = \tau_S(L) - \tau_S(L_0). \quad (14)$$

Assembling all intermediate results, we find for the reaction time

$$\tau_r(L) = \frac{\lambda(r_c)^{-1} + \tau_S(L_0, r_c)}{p_c(L, r_c)} + \frac{\Delta\tau_S(L)}{p_c(L, r_c)}, \quad (15)$$

$$= \tau_r(L_0) \frac{p_c(L_0, r_c)}{p_c(L, r_c)} + \frac{\Delta\tau_S(L)}{p_c(L, r_c)}. \quad (16)$$

The above reasoning holds true equally well for the true microscopic dynamics and the dynamics of a (coarse-grain)

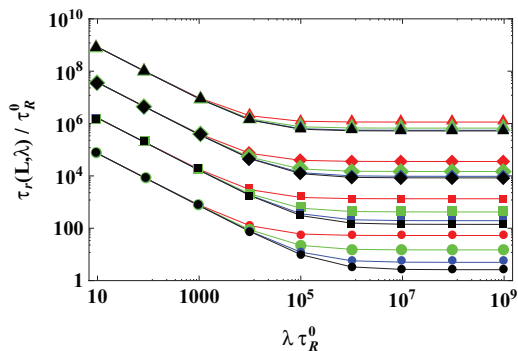


FIG. 6. Reaction times as a function of the chemical conversion rate, λ , for reactive sites in contact calculated from Eq. (2) for the systems in $d = 3$ presented in Fig. 4. Results are shown for four different chain lengths $L/L_0 = 1, 8, 64, 512$ from bottom to top. The color code denoting different discretizations of the chains is the same as in the preceding figures.

model describing the system. Equation (15) implies a few interesting consequences as follows:

- There are two distinct “polymer effects” on chemical reactivity: a static effect through the reduced contact probability in larger chains, $p_c(L_0, r_c)/p_c(L, r_c) \sim L^{dv}$ and a dynamic effect through the large-scale polymer motion.
- If the polymer dynamics is compact, the latter effect dominates asymptotically. Conversely, if the polymer dynamics is non-compact, the latter effect is negligible compared to the first one (see Eq. (8)).
- A polymer model, which faithfully describes the polymer dynamics and conformational statistics on scales larger than the reference chain, can be used to calculate $\frac{p_c(L_0, r_c)}{p_c(L, r_c)}$ and

$$\tau_S(L) - \tau_S(L_0) = \tau_S'(L) - \tau_S'(L_0), \quad (17)$$

where primed and unprimed symbols refer to model and the physical system, respectively.

- As we discuss in detail in Sec. IV D, it is possible to compensate the consequences of a modified short-time dynamics in a model by adjusting the reactivity parameters. In particular, changes of resolution can be performed without loss of predictive power, since the new values for r_c and λ are independent of chain length. The necessary matching of parameters can thus be carried out for reference chains of moderate lengths, which are still accessible to treatment in the more detailed model.

C. Coupling of contact radius and conversion rate

The decomposition of the process into the formation of a contact and a subsequent reaction is a theoretical abstraction with a somewhat arbitrary choice of r_c . In the simplest case, one should expect a distance dependent reaction rate. The probability for the occurrence of the reaction should then depend on the manner (compact/non-compact) in which the chain ends explore the reaction volume once they have entered into it. While this is an intriguing question, it requires a *microscopic* description of the reaction. Given that by constructing a polymer model we have already accepted to take some liberties with the microscopic structure and dynamics, we will allow ourselves to work with a modified, effective conversion rate, λ' , and with a modified, effective contact radius, r_c' under the minimal condition that the resulting reaction times, $\tau_r = \tau_{rc} + \tau_{dc}$, Eq. (2) remain unaffected. A general discussion on how to (best) preserve the *distribution* of reaction times is beyond the scope of the present paper.

Our approach is efficiently described with the help of Fig. 7. The figure shows the behavior of τ_{dc}/τ_R^0 as a function of r_c/R_0 , for the reference chain of contour length $L = L_0$ in $d = 3$. These results are obtained by numerical integration of Eq. (4) with Eqs. (6), (10), and (11). Different colors correspond to different spatial discretization of the reference chain. Consider now the horizontal line in Fig. 7 as indicating the (experimentally or numerically measured) reaction time of the

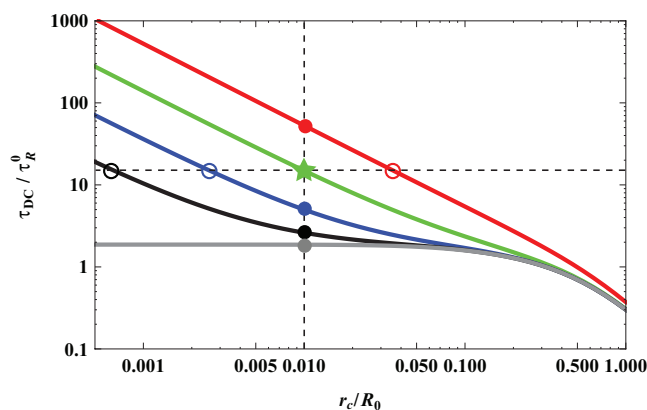


FIG. 7. Numerical results for τ_{dc}/τ_R^0 vs. r_c/R_0 (Eq. (4)), for the reference chain of contour length $L = L_0$ in $d = 3$. Different colors correspond to different discretizations of the reference chain: $N = N_0 = 4$ (red), $N_0 = 16$ (green), $N_0 = 64$ (blue), $N_0 = 256$ (black), while the grey line corresponds to the continuum chain limit ($N_0 \rightarrow \infty$). The “target” system is represented by the green chain: the specific “target” value $\tau_{dc}(r_c = r_c^*)$ with $r_c^*/R_0 = 0.01$ (the same as in Figs. 4 and 6) is marked by a green star, while corresponding values for different discretizations (at the same ratio r_c/R_0) are marked by filled circles. Alternatively, one can model the reaction by keeping fixed τ_{dc}/τ_R^0 , and adopt larger or smaller reaction radii in coarser or finer models, respectively (open circles).

reference chain. Choosing the *model-dependent* contact radii indicated by the open circles from the condition $\tau_{dc}(r_c^*) \equiv \tau_r$, the reaction time is reproduced with the choice $\lambda^{-1} = 0$ of an infinitely fast reaction for chain ends entering the contact volume.⁷ τ_r can also be reproduced by other choices of r_c , provided

$$\lambda(r_c)^{-1} = p_c(r_c)(\tau_r - \tau_{dc}(r_c)). \quad (18)$$

The required conversion rates are shown in Fig. 8. The behavior is quite intuitive: contact radii $r_c > r_c^*$ lead to reduced mean-first contact times. To correct for this, one has to choose a finite conversion rate $0 < \lambda < \infty$. For $r_c < r_c^*$ the mean-first contact times exceed the target reaction time. In this case, Eq. (18) leads to unphysical negative conversion rates.

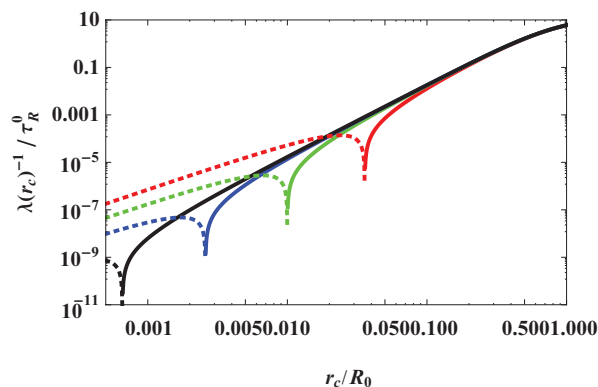


FIG. 8. Inverse of conversion rates $\lambda(r_c)^{-1}$ as a function of the contact radius, r_c (Eq. (18)) required in order to reproduce the “target” reaction time $\tau_r = \tau_{dc}(r_c^*)$ shown in Fig. 7. Dotted and solid portions of the curves correspond to negative or positive conversion rates, respectively. The color code denoting different discretizations of the chain is the same as in Fig. 7.

D. Reactivity parameters for models with different resolution

Now consider the problem of a polymeric system, whose behavior we wish to reproduce using models with different spatial resolution. The first strategy we explore is to keep r_c fixed across changes of resolution and to adjust λ in such a way that deviations in τ_{dc} are compensated by a suitably corrected τ_{rc} . Following the logic of the preceding section, the modified reaction rates are given by

$$\lambda'(r_c)^{-1} = \lambda(r_c)^{-1} + \tau_S(L_0, r_c) - \tau_S'(L_0, r_c). \quad (19)$$

The result as a function of r_c/R_0 is given in Fig. 9. We note that the necessary correction can be calculated and applied independently of the chemical conversion rate, $\lambda(r_c)$, at contact. In particular, $\Delta\tau_S' = \tau_S'(L_0, r_c) - \tau_S(L_0, r_c)$ can be determined for *small* systems, since the differences in the dynamics are independent of chain length and confined to microscopic time scales. With $\Delta\tau_S'$ faithfully removing model artifacts in the short-time contributions to $\tau_S(L)$, it may again have either sign, depending on whether the model neglects a regime of non-compact diffusion present in the true dynamics or whether the model introduces such a regime *not present* in the true dynamics. Typically, $\Delta\tau_S' > 0$ in the continuum limit preferred by theorists, while the omission of microscopic degrees of freedom in coarse-grain models can lead to $\Delta\tau_S' < 0$ (Fig. 9).

To illustrate this point, we reconsider our example of differently discretized Rouse chains from a new perspective. We choose the intermediate “green” systems with $N = 16(L/L_0)$ beads as targets whose behavior we wish to reproduce using the other Rouse models. As can be inferred from Fig. 4, $\tau_S'(L) - \tau_S(L)$ is essentially independent of chain length with $\Delta\tau_S' > 0$ and $\Delta\tau_S' < 0$ for models with a finer or a coarser discretization than the target system. By construction, target and models share the same large-scale and long-time behavior, but differ in the duration of the non-compact, diffusive regime in their short-time dynamics. Using the effective conversion

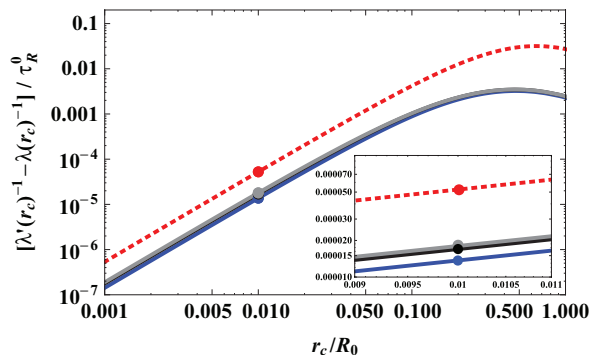


FIG. 9. Corrections to the reaction rates, $\lambda'(r_c)^{-1} - \lambda(r_c)^{-1}$ (Eq. (19)), which have to be adopted in polymer models corresponding to spatial discretizations shown in Fig. 7 (same color code), in order to reproduce the reaction times calculated for the reference chain with $N_0 = 16$ (Fig. 7, green system). The filled circles (see *inset* for a zoomed picture) show corrections corresponding to $r_c/R_0 = 0.01$ (see corresponding symbols in Fig. 7). Negative or positive corrections (corresponding to coarser or finer models) are indicated by dotted or solid lines, respectively.

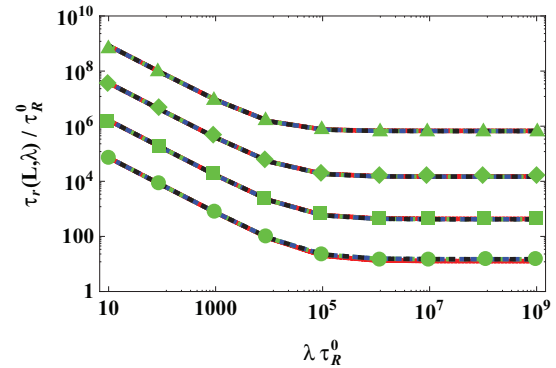


FIG. 10. Predictive power of models with different spatial resolution for a given value of r_c and reaction rates λ' adjusted according to Eq. (19) to match the “green” system in Fig. 6 at the reference chain length L_0 (bottom set of curves). The three remaining sets of curves and symbols show predictions for three different chain lengths $L/L_0 = 8, 64, 512$ (from bottom to top). The color code denoting different discretizations of the chains is the same as in the preceding figures.

rates, λ' from Eq. (19), the agreement between predictions from different models in Fig. 10 is now comparable to the viscosities presented in Fig. 5. Equation (19) looks innocent enough, but for $\Delta\tau_S' < 0$ its application formally leads to a divergence at $\lambda^{-1} + \Delta\tau_S' \equiv 0$ and to negative values for $\lim_{\lambda \rightarrow \infty} \lambda' = \Delta\tau_S'^{-1}$. But even if the regularized model parameters are difficult to interpret, the example of the dataset in Fig. 10 shows that the procedure is numerically well defined and can be used to *predict* reaction times from models with different spatial resolution.

As an alternative strategy, we can modify r_c to a different value r_c' in such a way that τ_{dc} remains constant for models with different spatial resolution. The modified λ' can then be derived by imposing that τ_{rc}/τ_R^0 does not change with chain spatial resolution, thus giving $\lambda' = \lambda'(r_c') = \lambda(r_c) \frac{p_c(r_c)}{p_c(r_c')}$. It is

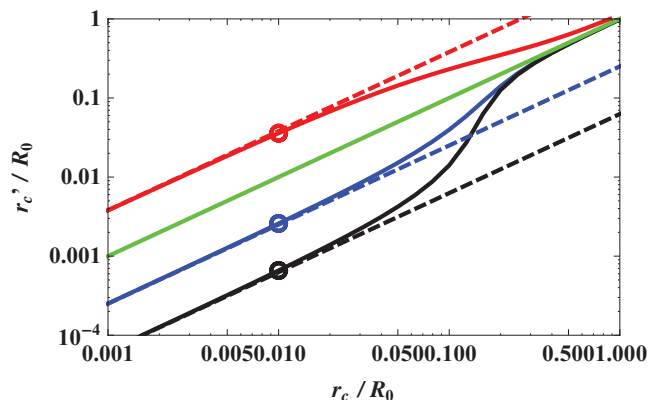


FIG. 11. Modified reaction radii $r_c' = r_c'(r_c)$ which have to be adopted in order to reproduce the diffusion-controlled reaction time τ_{dc}/τ_R^0 calculated for the “green” system with $N_0 = 16$ and reaction radius r_c (Fig. 7) by coarser (red solid line) or finer (blue and black solid lines) chains. The green line corresponds to $r_c' = r_c$. Dashed lines show the corresponding, exact results for small r_c/R_0 . Open circles mark the modified radii for $r_c/R_0 = 0.01$ (see corresponding symbols in Fig. 7). Notice, that modified contact radii found for the reference chain with $L = L_0$ predict the correct results for longer “target” chains (see Figs. 12 and 13).

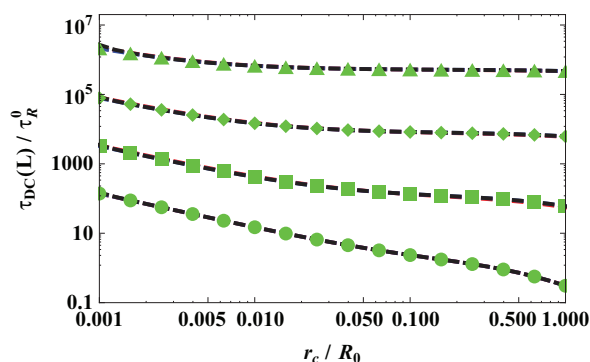


FIG. 12. Diffusion-controlled reaction times, $\tau_{dc}(L)$ as a function of the reaction radius, r_c of the “target” model ($N = 16(L/L_0)$, green symbols), for Rouse chains of contour length $L/L_0 = 1, 8, 64, 512$ (from bottom to top), in $d = 3$. By adopting the values $r_c' = r_c'(r_c)$ modified accordingly to the spatial resolution of the reference chain with $L = L_0$ (see Fig. 11), different spatial discretizations (overlapping dashed lines) faithfully reproduce the correct result. The color code denoting different discretizations of the chains is the same as in Fig. 7.

easy to verify that $r_c' = r_c'(r_c)$ grows with the smallest scale resolved in the employed model (solid lines, Fig. 11). For the Rouse model in $d > 2$, we find for small contact radii $r_c'/r_c = (b'/b)^{2(d-2)}$, where b and b' are the bond lengths of the corresponding Gaussian chains (dashed lines, Fig. 11).

To validate the predictive power of models with correspondingly adjusted reactivity parameters, we consider again the example of differently discretized Rouse chains, and we choose the intermediate “green” systems with $N = 16(L/L_0)$ beads as targets. Fig. 12 show plots of $\tau_{dc}(r_c)$ for $3d$ chains with different spatial discretizations and contour lengths $L/L_0 = 1, 8, 64, 512$ (from bottom to top). As in Fig. 10, we have adjusted the parameters for short reference chains of length L_0 and employed the same values of contact radii for chain lengths $L/L_0 \geq 8$. This same protocol is shown to work in higher dimensions as well (Fig. 13).

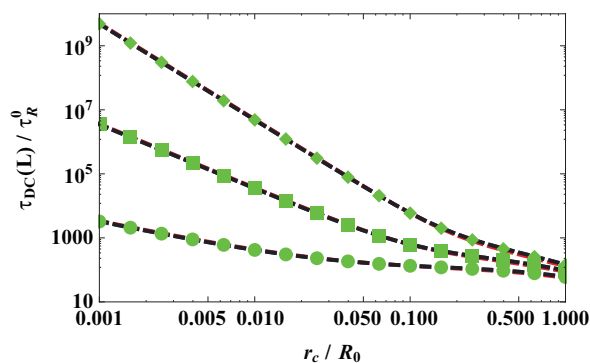


FIG. 13. Diffusion-controlled reaction times, $\tau_{dc}(L)$ as a function of the reaction radius, r_c of the “target” model ($N = 16(L/L_0)$, green symbols), for Rouse chains of contour length $L = 8L_0$, in $d = 3, 4, 5$ dimensions (from bottom to top). By adopting the values $r_c' = r_c'(r_c)$ modified accordingly to the spatial resolution of the shorter reference chain with $L = L_0$, different spatial discretizations (overlapping dashed lines) faithfully reproduce the correct result. The color code denoting different discretizations of the chains is the same as in Fig. 7.

While we prefer the second strategy for numerical studies with discrete models of different resolution, we note that analytical approaches employing the continuum limit need to include the effects of the local, short-time dynamics of real polymers in an effective conversion rate.

V. SUMMARY

Polymeric system may exhibit different dynamic regimes on different time and length scales.^{49–52} While complex, most of these properties can be reproduced by a hierarchy of models hiding molecular specificity in a small number of parameters accounting for the chain topology and conformational statistics or the effective interactions. In this context, we have taken a closer look at the prediction of diffusion-controlled reaction rates in polymeric systems. Our results are based on the formalism by Wilemski and Fixman¹ in an approximation proposed by Doi.⁵ Doi’s formulation focuses on the contact correlation time, τ_S , and provides useful physical insight into the factors controlling the result of the full solution of the Wilemski-Fixman theory. Here we build on the observation, that the short-time dynamics of polymers is independent of chain length. In particular, we propose to distinguish a *model-dependent, chain-length independent* short-time contribution, τ_S^{micro} , and a *universal, chain-length dependent* long-time contribution, $\tau_S^{\text{pol}}(L)$. The relative importance of these contributions depends on the local and the large-scale polymer dynamics and the compact/non-compact exploration^{7,8} of the reduced configuration space.

To illustrate our results, we have considered the well-known problem of chain cyclization.^{2,3,6} In particular, we have used the Rouse model, because it allows for a straightforward analytical calculation of the renormalisation of the model parameters, when the same system is considered with varying spatial resolution. For finite discretizations, the Rouse model exhibits two different dynamical regimes: free monomer diffusion at short times, and Rouse dynamics at large times. For $d < 4$ we find, that the asymptotically dominant $\sim L^2$ regime with $\tau_{dc}(L) \sim \tau_R(L)$ can be obtained with minimal corrections to scaling from $\tau_S^{\text{pol}}(L)$ and is a manifestation of the *compact*, large-scale polymer dynamics. In contrast, the asymptotically sub-dominant $L^{d/2}$ regime results from the reweighting of the chain-length independent contribution τ_S^{micro} with the chain-length dependent, *static* contact probability, $p_c \sim L^{-d/2}$. The value of τ_S^{micro} determines the importance of this regime and the chain length where the overall behavior crosses over to the L^2 -regime.¹³ Large values of τ_S^{micro} are due to short-time regimes in the local dynamics, which give rise to *non-compact* diffusion. In particular, the example of the Rouse model demonstrates a breakdown of the usual benign neglect of microscopic detail: by themselves (i) the knowledge of the (chemical) conversion rate for reactive sites in contact and (ii) a reliable model of the large-scale structure and dynamics are insufficient to predict reaction rates in diffusion-controlled processes. Contrary to quantities, such as the solution viscosity (Fig. 5), predictions for the contact correlation time τ_S , the diffusion-limited reaction time τ_{dc} , and the reaction

time τ_r (Eqs. (5), (4), and (2), respectively) may be strongly affected by the spatial resolution of the employed model (Figs. 4 and 6).

This potentially poses a serious problem to the development of *predictive* multi-scale modeling schemes for chemical diffusion-controlled reaction rates in polymers. Conceptually, it is not surprising that the microscopic reactivity parameters r_c and λ need to be adjusted upon a change of scale. After all, by constructing polymer models with different resolution, one inevitably sacrifices the precision of the representation of the microscopic structure and dynamics. In the present paper, we were able to show that the required changes are independent of chain length. The key is our identification of the *model-dependent*, but *chain-length independent* nature of the short-time contribution, τ_S^{micro} , to the contact correlation time, $\tau_S(L)$, and the resulting mean-first contact and reaction times, $\tau_{dc}(L)$ and $\tau_r(L)$. In Sec. IV D, we have discussed two simple schemes for choosing reactivity parameters r_c and λ such that they cancel the consequences of modifications in the local chain dynamics introduced in models with different spatial resolution. While the matching of τ_S^{micro} can be carried out for *short* reference chains, the procedure is *predictive* for long chains to the extent that the employed models correctly represent the large-scale polymer structure and dynamics and hence the *universal, chain-length dependent* long-time contribution, $\tau_S^{\text{pol}}(L)$. While we have used the Rouse model to illustrate our results, we emphasize that quantitatively different, but conceptually similar problems need to be dealt with in all attempts to predict chemical reaction times in polymeric systems from (a hierarchy of) models.

APPENDIX A: ROUSE MODEL IN d -DIMENSIONS

In the Rouse model,^{45,46} the polymer chain is described as a linear array of $N + 1$ beads connected by Gaussian springs with Hamiltonian given by

$$\mathcal{H} = \frac{k}{2} \sum_{n=0}^{N-1} (\vec{r}_{n+1} - \vec{r}_n)^2. \quad (\text{A1})$$

In Eq. (A1), \vec{r}_n is the spatial position of the n th bead (numbered from one chosen end of the chain), $k = d N k_B T / R^2$ and $R^2 = \langle (\vec{r}_N - \vec{r}_0)^2 \rangle$ is the mean-square end-to-end distance. Traditionally,^{45,46} one assumes the same friction coefficient, $\zeta_n \equiv \zeta$ for all monomers. This leads to the (asymptotically irrelevant) complication, that the length of the chain scales with the number of bonds, N , while the center of mass friction scales with the number of beads, $N + 1$. As an alternative, we propose to represent sections of a real polymer by a (Rouse) dumbbell with half of the total friction concentrated in each bead and an appropriate entropic spring representing the integrated-out degrees of freedom. For a (Rouse) chain composed of N such segments, the monomer friction coefficients are given by: $\zeta_n \equiv \zeta$ for $1 \leq n \leq N - 1$ and $\zeta_0 = \zeta_N \equiv \zeta/2$.

According to the Rouse model, the time evolution of spatial positions $\vec{r}_n(t)$ is described by the Langevin equations

$$\begin{aligned} \zeta_0 \dot{\vec{r}}_0(t) &= -k[\vec{r}_0(t) - \vec{r}_1(t)] + \vec{f}_0(t), \\ \zeta_n \dot{\vec{r}}_n(t) &= -k[2\vec{r}_n(t) - \vec{r}_{n+1}(t) - \vec{r}_{n-1}(t) \\ &\quad + \vec{f}_n(t)], \quad 1 \leq n \leq N - 1, \\ \zeta_N \dot{\vec{r}}_N(t) &= -k[\vec{r}_N(t) - \vec{r}_{N-1}(t)] + \vec{f}_N(t), \end{aligned} \quad (\text{A2})$$

where the Gaussian random forces $\vec{f}_n(t)$ satisfy $\langle \vec{f}_n(t) \rangle = 0$ and $\langle \vec{f}_m(t) \times \vec{f}_n(t') \rangle = 2d \zeta_n k_B T \delta_{mn} \delta(t - t')$. By defining the eigen-modes^{45,46} $\vec{X}_p(t)$ ($0 \leq p \leq N$) of the Rouse chain as

$$\vec{X}_p(t) = \frac{1}{N} \left[\frac{1}{2} \vec{r}_0(t) + \sum_{n=1}^{N-1} \vec{r}_n(t) \cos\left(\frac{p\pi n}{N}\right) + \frac{(-1)^p}{2} \vec{r}_N(t) \right], \quad (\text{A3})$$

Eq. (A2) reduces to the following simple linear equations for the modes:

$$\zeta_p \dot{\vec{X}}_p(t) = -k_p \vec{X}_p(t) + \vec{f}_p(t) \quad (0 \leq p \leq N), \quad (\text{A4})$$

with

$$k_p = 2k \frac{\zeta_p}{\zeta} \left[1 - \cos\left(\frac{p\pi}{N}\right) \right] \quad (\text{A5})$$

and

$$\zeta_p = \begin{cases} N\zeta, & \text{if } p = 0 \text{ and } p = N \\ 2N\zeta, & \text{if } 1 \leq p \leq N - 1 \end{cases}, \quad (\text{A6})$$

and corresponding statistical correlations $\langle \vec{f}_p(t) \rangle = 0$ and $\langle \vec{f}_p(t) \times \vec{f}_q(t') \rangle = 2d \zeta_p k_B T \delta_{pq} \delta(t - t')$. Hence, the time correlation function $\langle \vec{X}_p(t) \times \vec{X}_q(0) \rangle$ is equal to

$$\langle \vec{X}_p(t) \times \vec{X}_q(0) \rangle = d \delta_{pq} \frac{k_B T}{k_p} \exp\left(-\frac{t}{\tau_p}\right), \quad (\text{A7})$$

where

$$\tau_p = \frac{\zeta_p}{k_p} = \tau_1 \frac{1 - \cos\left(\frac{\pi}{N}\right)}{1 - \cos\left(\frac{p\pi}{N}\right)}, \quad (\text{A8})$$

and $\tau_1 = \zeta / (2k [1 - \cos(\frac{\pi}{N})]) = \tau_R$ is the Rouse time of the chain.

Spatial monomer vectors $\vec{r}_n(t)$ can be expressed in terms of Rouse modes, Eq. (A3) as

$$\vec{r}_n(t) = \vec{X}_0(t) + 2 \sum_{p=1}^{N-1} \vec{X}_p(t) \cos\left(\frac{p\pi n}{N}\right) + (-1)^n X_N(t), \quad (\text{A9})$$

so that the end-to-end vector $\vec{r}(t) \equiv \vec{r}_N(t) - \vec{r}_0(t)$ of the chain is given by

$$\vec{r}(t) = \begin{cases} -4 \sum_{p=1, \text{odd}}^{N-1} \vec{X}_p(t), & \text{if } N \text{ even} \\ -4 \sum_{p=1, \text{odd}}^{N-2} \vec{X}_p(t) - 2X_N(t), & \text{if } N \text{ odd} \end{cases}. \quad (\text{A10})$$

Finally, the time correlation function, $\phi(t) \equiv \langle \vec{r}(t) \cdot \vec{r}(0) \rangle / \langle \vec{r}(0)^2 \rangle$ can be obtained from the mode cross-correlation expression, Eq. (A7),

$$\phi(t) = \begin{cases} \frac{4}{N^2} \sum_{p=1; \text{odd}}^{N-1} \frac{\exp\left(-\frac{t}{\tau_p}\right)}{1 - \cos\left(\frac{p\pi}{N}\right)}, & \text{if } N \text{ even} \\ \frac{1}{N^2} \left[4 \sum_{p=1; \text{odd}}^{N-2} \frac{\exp\left(-\frac{t}{\tau_p}\right)}{1 - \cos\left(\frac{p\pi}{N}\right)} + \exp\left(-\frac{t}{\tau_N}\right) \right], & \text{if } N \text{ odd} \end{cases} \quad (\text{A11})$$

In this work due to its more compact expression, we have considered only the case corresponding to even N 's.

APPENDIX B: CONTACT CORRELATION FUNCTION FOR THE ROUSE MODEL

We can now derive the contact correlation function, $\Sigma(t)$, Eq. (9), for the Rouse model. In d -dimensions, the required Green's function $G(\vec{r}, t|\vec{r}_0, 0)$ is given by the *exact* expression,²

$$G(\vec{r}, t|\vec{r}_0, 0) = \left(\frac{d}{2\pi R^2[1 - \phi^2(t)]} \right)^{d/2} \times \exp\left(-\frac{d}{2R^2} \frac{[\vec{r} - \phi(t)\vec{r}_0]^2}{[1 - \phi^2(t)]} \right). \quad (\text{B1})$$

It is easy to verify that: (1) $\lim_{t \rightarrow 0} G(\vec{r}, t|\vec{r}_0, 0) = \delta(\vec{r} - \vec{r}_0)$ and (2) $\lim_{t \rightarrow \infty} G(\vec{r}, t|\vec{r}_0, 0) = p_L(\vec{r}) = (d/2\pi R^2)^{d/2} \exp(-d\vec{r}^2/2R^2)$.

In order to calculate $\Sigma(t)$ from Eq. (9), the sink function $S(\vec{r})$ has to be specified. Here, we discuss three functional forms, which were also discussed in the past:^{2,11}

1. The delta sink $S_\delta(\vec{r})$,

$$S_\delta(\vec{r}) = V_d(r_c) \delta(\vec{r}). \quad (\text{B2})$$

2. The Heaviside sink $S_H(\vec{r})$ with cubic symmetry

$$S_H(\vec{r}) = \begin{cases} 1, & \text{if } \vec{r} \in \left[-\frac{1}{2} (V_d(r_c))^{1/d}, +\frac{1}{2} (V_d(r_c))^{1/d} \right]^d \\ 0, & \text{otherwise} \end{cases}. \quad (\text{B3})$$

Wilemski and Fixman originally studied the corresponding Heaviside sink with *spherical* symmetry, and in $d = 3$ only.² While our ansatz, Eq. (B3) does not modify the underlying physics, it is computationally convenient in general d 's, as one only needs to calculate one-dimensional integrals.

3. The Gaussian sink $S_G(\vec{r})$,

$$S_G(\vec{r}) = \exp\left(-\frac{\pi \vec{r}^2}{(V_d(r_c))^{2/d}} \right). \quad (\text{B4})$$

This sink was originally proposed by Doi³ as a mathematically more convenient form than the spherically symmetric Heaviside sink.

For a given contact radius r_c , $V_d(r_c)$ is the d -dimensional, (hyper)spherical contact volume given by $V_d(r_c) = \frac{\pi^{d/2}}{\Gamma(d/2+1)} r_c^d$, where $\Gamma(x)$ is the Euler Gamma func-

tion. Then, Eq. (B2) implies that

$$p_{c,\delta}(r_c) = V_d(r_c) p_L(0), \quad (\text{B5})$$

while the adoptions of the Heaviside (B3) and the Gaussian sinks (B4) lead to, respectively,

$$p_{c,H}(r_c) = \left\{ \text{erf} \left[\frac{\pi^{1/2}}{2} (p_{c,\delta}(r_c))^{1/d} \right] \right\}^d \quad (\text{B6})$$

and

$$p_{c,G}(r_c) = \frac{p_{c,\delta}(r_c)}{(1 + (p_{c,\delta}(r_c))^{2/d})^{d/2}}, \quad (\text{B7})$$

where $\text{erf}(y) = \frac{2}{\pi^{1/2}} \int_0^y e^{-x^2} dx$ is the error function. Equations (B5)–(B7) imply immediately, that in the limit $r_c \rightarrow 0$ $p_{c,H}(r_c) \approx p_{c,G}(r_c) \approx p_{c,\delta}(r_c)$. Conversely, for a given contact probability p_c the contact radius corresponding to sinks Eqs. (B2)–(B4) is given, respectively, by

$$r_{c,\delta}(p_c) = \frac{1}{\pi^{1/2}} \left[\Gamma(d/2 + 1) \frac{p_c}{p_L(0)} \right]^{1/d}, \quad (\text{B8})$$

$$r_{c,H}(p_c) = \frac{2}{\pi^{1/2}} \frac{\text{erf}^{-1}(p_c^{1/d})}{p_c^{1/d}} r_{c,\delta}(p_c), \quad (\text{B9})$$

where $\text{erf}^{-1}(x)$ is the inverse of the error function, and

$$r_{c,G}(p_c) = \frac{r_{c,\delta}(p_c)}{\sqrt{1 - p_c^{2/d}}}. \quad (\text{B10})$$

Some care needs to be taken, when evaluating Eq. (9), since the sink function appears twice. In the following, we will use a notation where the result for $\Sigma(t)$ following the substitutions $S(\vec{r}) = S_a(\vec{r})$ and $S(\vec{r}_0) = S_b(\vec{r}_0)$ is denoted by $\Sigma_{a,b}$.

The problem becomes immediately apparent in the case

$$\Sigma_{\delta,\delta}(t) = \frac{p_c}{[1 - \phi^2(t)]^{d/2}}, \quad (\text{B11})$$

where the limit for $t \rightarrow 0$ is ill-defined. ‘‘Unbalanced’’² combinations of the Gaussian and the Heaviside sinks can be calculated analytically, giving respectively,

$$\Sigma_{G,\delta}(t) = \frac{p_c}{[(1 - p_c^{2/d})(1 - \phi^2(t)) + p_c^{2/d}]^{d/2}} \quad (\text{B12})$$

and

$$\Sigma_{H,\delta}(t) = \left\{ \text{erf} \left[\frac{\text{erf}^{-1}(p_c^{1/d})}{\sqrt{1 - \phi^2(t)}} \right] \right\}^d. \quad (\text{B13})$$

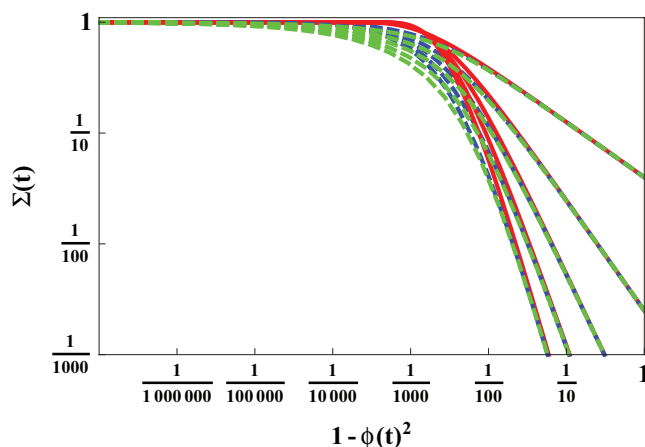


FIG. 14. Comparison between the exact expressions for $\Sigma_{H,\delta}(t)$ (Eq. (B13), red solid line), $\Sigma_{G,\delta}(t)$ (Eq. (B12), blue dashed line), and the numerical evaluated $\Sigma_{H,H}(t)$ (green dashed line), as a function of $1 - \phi^2(t)$ for $r_c/R = 0.05$ in $d = 1$ to 5 dimensions (from top to bottom). These expressions deviate around $1 - \phi^2(t) \approx (r_c/R)^2$, i.e., when the interacting particles reach the sink boundaries.

It is easy to verify that Eqs. (B12) and (B13) both satisfy the requested constraints (Sec. II A): $\Sigma(t \rightarrow 0) = 1$ and $\Sigma(t \rightarrow \infty) = p_c$. It is also possible to define a variant of the Gaussian sink, which fulfills $\langle S_G \rangle = \langle S_G^2 \rangle$ for Gaussian chains with $p_L(\vec{r}) = (d/2\pi R^2)^{d/2} \exp(-d\vec{r}^2/2R^2)$, leading to $\Sigma_{G,G} = \Sigma_{G,\delta}$.

Figure 14 compares $\Sigma_{G,\delta}(t)$, $\Sigma_{H,\delta}(t)$ and the numerically determined $\Sigma_{H,H}(t)$. We notice that these expressions show some deviations around $1 - \phi^2(t) \approx (r_c/R)^2$. This is easily explained: for $\Sigma_{G,\delta}(t)$ and $\Sigma_{H,\delta}(t)$ the particles start at $\vec{r} = 0$ and they need a finite amount of time in order to reach the boundaries of the interaction region. For our present purposes, the choice between the different functional forms is mainly a matter of computational convenience and we have, therefore, used the simpler form Eq. (B12).

¹G. Wilemski and M. Fixman, *J. Chem. Phys.* **60**, 866 (1974).

²G. Wilemski and M. Fixman, *J. Chem. Phys.* **60**, 878 (1974).

³M. Doi, *Chem. Phys.* **9**, 455 (1975).

⁴M. Doi, *Chem. Phys.* **11**, 107 (1975).

⁵M. Doi, *Chem. Phys.* **11**, 115 (1975).

⁶A. Szabo, K. Schulten, and Z. Schulten, *J. Chem. Phys.* **72**, 4350 (1980).

⁷P.-G. de Gennes, *J. Chem. Phys.* **76**, 3316 (1982).

⁸P.-G. de Gennes, *J. Chem. Phys.* **76**, 3322 (1982).

⁹B. Friedman and B. O'Shaughnessy, *Phys. Rev. Lett.* **60**, 64 (1988).

¹⁰B. Friedman and B. O'Shaughnessy, *Phys. Rev. A* **40**, 5950 (1989).

¹¹R. W. Pastor, R. Zwanzig, and A. Szabo, *J. Chem. Phys.* **105**, 3878 (1996).

¹²S. Jun, J. Bechhoefer, and B.-Y. Ha, *Europhys. Lett.* **64**, 420 (2003).

¹³J. Z. Y. Chen, H.-K. Tsao, and Y.-J. Sheng, *Phys. Rev. E* **72**, 031804 (2005).

¹⁴N. M. Toan, D. Marenduzzo, P. R. Cook, and C. Micheletti, *Phys. Rev. Lett.* **97**, 178302 (2006).

¹⁵I. M. Sokolov, *Phys. Rev. Lett.* **90**, 080601 (2003).

¹⁶A. E. Likhtman and C. M. Marques, *Europhys. Lett.* **75**, 971 (2006).

¹⁷N. M. Toan, G. Morrison, C. Hyeon, and D. Thirumalai, *J. Phys. Chem. B* **112**, 6094 (2008).

¹⁸S. H. Northrup, S. A. Allison, and J. A. McCammon, *J. Chem. Phys.* **80**, 1517 (1984).

¹⁹F. A. Escobedo, E. E. Borrero, and J. C. Araque, *J. Phys.: Condens. Matter* **21**, 333101 (2009).

²⁰G. A. Huber and J. A. McCammon, *Comput. Phys. Commun.* **181**, 1896 (2010).

²¹Q. Du, C. Smith, N. Shiffeldrim, M. Vologodskiaia, and A. Vologodskii, *Proc. Natl. Acad. Sci. U.S.A.* **102**, 5397 (2005).

²²T. E. Cloutier and J. Widom, *Proc. Natl. Acad. Sci. U.S.A.* **102**, 3645 (2005).

²³S. J. Hagen, C. W. Carswell, and E. M. Sjolander, *J. Mol. Biol.* **305**, 1161 (2001).

²⁴R. R. Hudgins, F. Huang, G. Gramlich, and W. M. Nau, *J. Am. Chem. Soc.* **124**, 556 (2002).

²⁵L. J. Lapidus, W. A. Eaton, and J. Hofrichter, *Proc. Natl. Acad. Sci. U.S.A.* **97**, 7220 (2002).

²⁶L. J. Lapidus, P. J. Steinbach, W. A. Eaton, A. Szabo, and J. Hofrichter, *J. Phys. Chem. B* **106**, 11628 (2002).

²⁷I.-J. Chang, J. C. Lee, J. R. Winkler, and H. B. Gray, *Proc. Natl. Acad. Sci. U.S.A.* **100**, 3838 (2003).

²⁸H. Neuweiler, A. Schulz, M. Bohmer, J. Enderlein, and M. Sauer, *J. Am. Chem. Soc.* **125**, 5324 (2003).

²⁹H. Sahoo, D. Roccatano, M. Zacharias, and W. M. Nau, *J. Am. Chem. Soc.* **128**, 8118 (2006).

³⁰J. C. Lee, B. T. Lai, J. J. Kozak, H. B. Gray, and J. R. Winkler, *J. Phys. Chem. B* **111**, 2107 (2007).

³¹D. Shore and R. L. Baldwin, *J. Mol. Biol.* **170**, 957 (1983).

³²D. Thirumalai and C. Hyeon, *Biochemistry* **44**, 4957 (2005).

³³M. Murat and K. Kremer, *J. Chem. Phys.* **108**, 4340 (1998).

³⁴J. Baschnagel, K. Binder, P. Doruker, A. A. Gusev, O. Hahn, K. Kremer, W. L. Mattice, F. Müller-Plathe, M. Murat, W. Paul, S. Santos, U. W. Suter, and V. Triess, *Adv. Polym. Sci.* **152**, 41 (2000).

³⁵F. Eurich and P. Maass, *J. Chem. Phys.* **114**, 7655 (2001).

³⁶V. A. Harmandaris, N. P. Adhikari, N. F. A. van der Vegt, and K. Kremer, *Macromolecules* **39**, 6708 (2006).

³⁷C. Pierleoni, C. Addison, J.-P. Hansen, and V. Krakoviack, *Phys. Rev. Lett.* **96**, 128302 (2006).

³⁸J. Ramirez, S. K. Sukumaran, and A. E. Likhtman, *Macromol. Symp.* **252**, 119 (2007).

³⁹C. Pierleoni, B. Capone, and J.-P. Hansen, *J. Chem. Phys.* **127**, 171102 (2007).

⁴⁰*Coarse-Graining of Condensed Phase and Biomolecular Systems*, edited by G. A. Voth (CRC, London, 2008).

⁴¹V. Rühle, C. Junghans, A. Lukyanov, K. Kremer, and D. Andrienko, *J. Chem. Theory Comput.* **5**, 3211 (2009).

⁴²Y. von Hansen, R. R. Netz, and M. Hinczewski, *J. Chem. Phys.* **132**, 135103 (2010).

⁴³J. Ramirez, S. K. Sukumaran, B. Vorselaar, and A. E. Likhtman, *J. Chem. Phys.* **133**, 154103 (2010).

⁴⁴M. Smoluchowski, *Z. Phys. Chem.* **92**, 129 (1917).

⁴⁵P. E. Rouse, *J. Chem. Phys.* **21**, 1272 (1953).

⁴⁶M. Doi and S. F. Edwards, *The Theory of Polymer Dynamics* (Oxford University Press, New York, 1986).

⁴⁷M. Rubinstein and R. H. Colby, *Polymer Physics* (Oxford University Press, New York, 2003).

⁴⁸B. H. Zimm, *J. Chem. Phys.* **24**, 269 (1956).

⁴⁹E. Farge and A. C. Maggs, *Macromolecules* **26**, 5041 (1993).

⁵⁰R. Everaers, F. Julicher, A. Ajdari, and A. C. Maggs, *Phys. Rev. Lett.* **82**, 3717 (1999).

⁵¹P. Ahlrichs and B. Dunweg, *J. Chem. Phys.* **111**, 8225 (1999).

⁵²O. Hallatschek, E. Frey, and K. Kroy, *Phys. Rev. Lett.* **94**, 077804 (2005).

⁵³C. Yeung and B. Friedman, *J. Chem. Phys.* **122**, 214909 (2005).

⁵⁴P.-G. de Gennes, *Scaling Concepts in Polymer Physics* (Cornell University Press, Ithaca, 1979).

⁵⁵P. J. Flory, *Statistical Mechanics of Chain Molecules* (Interscience, New York, 1969).

⁵⁶A. Y. Grosberg and A. R. Khokhlov, *Statistical Physics of Macromolecules* (AIP, New York, 1994).

⁵⁷See supplementary material at <http://dx.doi.org/10.1063/1.3673444> for the figure showing quantitative agreement between contact times calculated according to the Doi's approximation and numerical results by Pastor *et al.* (Ref. 11).

⁵⁸G. Wilemski and M. Fixman, *J. Chem. Phys.* **58**, 4009 (1973).